WALAILAK JOURNAL
http://wjst.wu.ac.th Engineering and Physical Sciences

MHD Coupled-Flow due to Oscillatory Motion of a Wall in a Channel Partially Filled by a Porous Medium with Hall Effect

Dileep Singh CHAUHAN[*] and Rashmi AGRAWAL

Department of Mathematics, University of Rajasthan, Jaipur 302004, India

([*]Corresponding author's e-mail: dileepschauhan@gmail.com)

Abstract

This study aims to investigate the Hall effect on an unsteady flow in a composite channel of an upper oscillating wall in the presence of an inclined magnetic field. The flow field considered in the channel is composed of porous medium and clear viscous layers. The governing equations for flow and magnetic field are solved numerically by the Crank-Nicolson implicit finite-difference scheme. The results obtained are discussed graphically for various values of the pertinent parameters.

Keywords: Unsteady flow, composite channel, porous medium, Hall effect, inclined magnetic field

Introduction

The transport of viscous fluids in the presence of porous media is a problem of wide ranging interest. The study of channels filled or partially filled with porous medium has received considerable attention because of its importance in various engineering and industrial settings, such as chemical dispensing through porous media, filtration process, drawing systems, and ground water hydrology. Associated heat transfer problems in such channels have gained extensive attention due to their applications in recent technology, for example, in improving the performance of heat exchangers, energy storage units such as solar collectors, chemical reactors, cooling equipments, and in designing the heating and ventilating systems of buildings. Extensive research work has been carried out in recent years to study various kinds of effects on flow and heat transfer in such channels. Beckermann *et al*. [1] investigated natural convection flow between a viscous fluid and a porous layer in a rectangular duct. Chang and Chang [2] studied mixed convection flow in a vertical channel partially filled with a porous medium. Haddad [3] investigated the effects of free convection in a vertical channel partially filled with a porous medium, while Alkam *et al*. [4] studied forced convection in such channels. Al-Nimr and Khadrawi [5] examined transient free convection effects in domains filled partially with porous substrates.

The Couette flow in a parallel-plate channel, in which one wall is a stationary plate and the other is moving or oscillating in its own plane, is one of the important fluid flow situations in engineering applications. Oscillatory forcing flow through porous medium, e.g. forcing in the form of sinusoidal oscillations, can be employed in enhanced oil recovery processes. Nakayama [6] presented analytical solutions for various situations of the Couette flow in a porous medium saturated with an inelastic non-Newtonian fluid, modeled by the Brinkman Forchheimer extension of the Darcy equation. Chauhan and Shekhawat [7], Chauhan and Vyas [8] examined the Couette flow of a compressible Newtonian fluid in the presence of a naturally permeable wall. Kuznetsov [9] studied the Couette flow and heat transfer in a parallel-plate channel partially filled by a porous medium using the Brinkman Forchheimer extension of the Darcy equation and the fluid-porous interface matching conditions suggested by Ochoa-Tapia and Whittaker [10,11]. The Couette flow, with slip and jump boundary conditions, was investigated by Marques *et al*. [12]. The effects of slip condition on the Stokes flow, and also on the Couette flow, due to one wall oscillating in its own plane and the other one being stationary in a horizontal channel, were investigated by Khaled and Vafai [13]. Bég *et al*. [14] studied the transient Couette flow using a network

simulation method in a non-Darcian porous medium rotating channel. Guria *et al*. [15] studied the oscillatory Couette flow in the presence of an inclined magnetic field. Chauhan and Kumar [16] examined heat transfer effects in a Couette flow through a channel partially filled with a porous medium in the presence of a heat source and transverse sinusoidal injection velocity. Chauhan and Kumar [17] investigated radiation effects in an oscillatory flow through a horizontal channel partially filled with a porous medium.

In recent years, electrically conducting viscous fluid transport through porous media in the presence of a magnetic field has increasingly become an attractive research field for several engineers in many diversified areas. Such magnetohydrodynamic (MHD) flows occur, for example, in the solidification process in metallurgy, in MHD power generators, in geophysics, and in some astrophysical problems. Modeling the effect of a magnetic field in flows through porous media was discussed by McWhirter *et al*. [18,19], by Nield [20], and by Geindreau and Auriault [21] in detail. MHD convection flow through porous medium in a rotating channel was studied by Krishna *et al*. [22]. Effects of magnetic field on non-Newtonian fluid flows in channels filled with a porous medium were investigated by Hayat *et al*. [23-26]. Bég *et al*. [27] presented a numerical study of MHD viscous flow in a rotating porous medium with the Hall current. Effects of the Hall current in MHD flows and heat transfer in rotating channels partially filled by a porous medium were investigated by Chauhan and Rastogi [28], and Chauhan and Agrawal [29,30]. Such effects are likely to be important in many industrial applications, such as, in MHD accelerators and generators, and in several geophysical and astrophysical situations.

In this paper, the unsteady flow of an electrically conducting viscous incompressible fluid through a horizontal channel partially filled with a porous medium is investigated with the Hall effect, in the presence of an inclined magnetic field. The flow in the channel is caused by an oscillatory motion of the upper impermeable plate. The initial boundary value problem is solved numerically by the Crank-Nicolson implicit finite difference scheme, and the effects of the pertinent parameters on the velocity field, shear stresses, and magnetic field are obtained and discussed graphically.

Formulation of problem

An unsteady flow of a viscous incompressible electrically conducting fluid through a parallel plate composite channel is considered. The channel walls are impermeable, electrically non-conducting, and separated by a distance 'd'. A highly porous layer of thickness 'a' is perfectly attached to the lower channel wall. A Cartesian coordinate system is assumed, with *x*-axis and *y*-axis lying on the lower bottom impermeable plate of the channel, and *z*-axis normal to it (see **Figure 1**). The fluid in the composite channel and the channel plates are initially at rest. At time $t' > 0$, the upper impermeable plate located at $z = d$ is given oscillatory motion in its own plane with a velocity $U_0 \cos \omega' t'$ and a uniform strong magnetic field H_0 is applied at an angle θ from normal direction of the channel. The flow in the channel is induced by this upper oscillatory plate. In the present study, the Hall effect is also considered since, for a strong applied magnetic field, it becomes significant.

The channel walls are taken as being infinite along *x* and *y* directions, so all physical quantities are assumed to be functions of *z* and *t* only. In the channel, flow field is divided into 2 regions;

Region-I, $(a' \le z \le d)$, clear fluid region and

Region-II, $(0 \le z \le a')$, porous medium region.

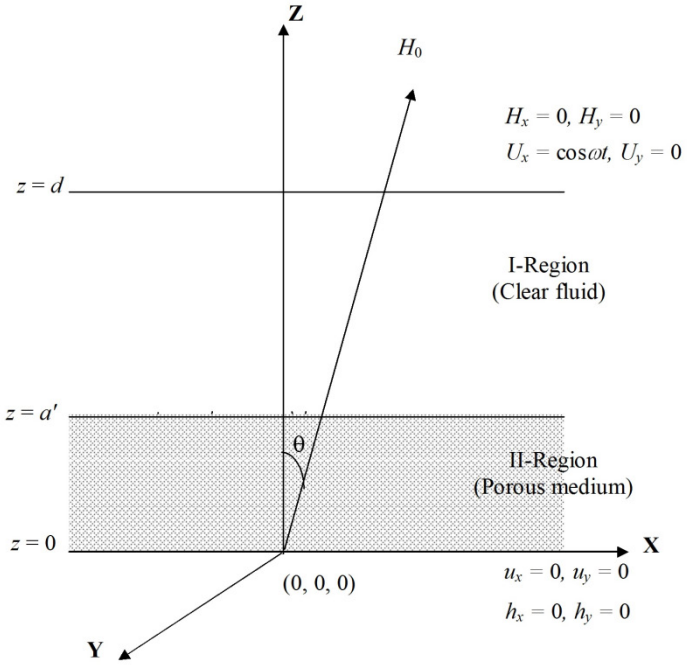

Figure 1 Schematic diagram.

The governing magnetohydrodynamic equations, Maxwell equations and the generalized Ohm's law, neglecting ion-slip and thermoelectric effect (Cowling [31]) are given by;

$$\nabla \cdot \boldsymbol{q}_i = 0\,, \tag{1}$$

$$\rho \frac{\partial \boldsymbol{q}_i}{\partial t'} + \rho\left(\boldsymbol{q}_i \cdot \nabla\right)\boldsymbol{q}_i = -\nabla p_i + \phi_i \nabla^2 \boldsymbol{q}_i + \mu_e \boldsymbol{J}_i \times \boldsymbol{H}_i - \frac{n\mu \boldsymbol{q}_i}{k_0}\,, \tag{2}$$

$$\nabla \cdot \boldsymbol{B}_i = 0\,, \tag{3}$$

$$\nabla \times \boldsymbol{E}_i = \text{-}\mu_e \frac{\partial \boldsymbol{H}_i}{\partial t'}\,, \tag{4}$$

$$\nabla \times \boldsymbol{H}_i = \boldsymbol{J}_i\,, \tag{5}$$

$$\nabla \cdot \boldsymbol{J}_i = 0\,, \tag{6}$$

$$\boldsymbol{J}_i + \frac{m}{H_0}\left(\boldsymbol{J}_i \times \boldsymbol{H}_i\right) = \sigma\left(\boldsymbol{E}_i + \mu_e \boldsymbol{q}_i \times \boldsymbol{H}_i\right), \tag{7}$$

where, for $i = 1,\ n = 0$, the above equations correspond to region-I; for $i = 2,\ n = 1$, the above equations correspond to region-II; for $i = 1,\ \phi_1 = \mu,$ viscosity of the fluid; for $i = 2,\ \phi_2 = \overline{\mu},$ effective viscosity of

the fluid in porous medium; $B_i = \mu_e H_i$, the magnetic induction; $m = \tau_e \omega_e$, the Hall current parameter; ρ, the fluid density; μ_e, the magnetic permeability; σ, the electrical conductivity; ω_e, the cyclotron frequency; τ_e, the electron collision time; k_0, the permeability of the porous medium; p_i, the pressure; and t', the time.

For $i = 1, 2$, let the velocity vector $\boldsymbol{q}_i$ be written as;

$$\boldsymbol{q}_1 = \left(U_x', U_y', 0\right),\ \boldsymbol{q}_2 = \left(u_x', u_y', 0\right);$$

the magnetic field $\boldsymbol{H}_i$ as;

$$\boldsymbol{H}_1 = \left(H_x' + H_0 \cos\theta, H_y', H_0 \sin\theta\right),\ \boldsymbol{H}_2 = \left(h_x' + H_0 \cos\theta, h_y', H_0 \sin\theta\right);$$

the electric field $\boldsymbol{E}_i$ as;

$$\boldsymbol{E}_1 = \left(E_x, E_y, E_z\right),\ \boldsymbol{E}_2 = \left(\bar{E}_x, \bar{E}_y, \bar{E}_z\right);$$

and the current density vector $\boldsymbol{J}_i$ as;

$$\boldsymbol{J}_1 = \left(J_x, J_y, 0\right),\ \boldsymbol{J}_2 = \left(\bar{J}_x, \bar{J}_y, 0\right),$$

for clear fluid region-I and the porous region-II, respectively.

Further, for partially ionized gases, the electron pressure gradient in Eq. (7) is neglected.

Using the above defined quantities, the initial and boundary conditions for the present problem are given by;

$$\text{For } t' \le 0, \quad U_x' = U_y' = 0, \quad H_x' = H_y' = 0, \quad u_x' = u_y' = 0, \quad h_x' = h_y' = 0 \quad \text{for all } z \tag{8}$$

$$\text{For } t' > 0, \quad \text{at } z = 0, \quad u_x' = u_y' = 0, \quad h_x' = h_y' = 0 \tag{9}$$

$$\text{at } z = a', \quad u_x' = U_x', \quad \bar{\mu}\frac{\partial u_x'}{\partial z} = \mu\frac{\partial U_x'}{\partial z}, \quad u_y' = U_y', \quad \bar{\mu}\frac{\partial u_y'}{\partial z} = \mu\frac{\partial U_y'}{\partial z} \tag{10}$$

$$h_x' = H_x', \quad \frac{\partial h_x'}{\partial z} = \frac{\partial H_x'}{\partial z}, \quad h_y' = H_y', \quad \frac{\partial h_y'}{\partial z} = \frac{\partial H_y'}{\partial z} \tag{11}$$

$$\text{at } z = d, \quad U_x' = U_0 \cos\omega' t', \quad U_y' = 0, \quad H_x' = H_y' = 0 \tag{12}$$

The following non-dimensional quantities are introduced:

$$U_x = \frac{U_x'}{U_0}, \qquad U_y = \frac{U_y'}{U_0}, \tag{13}$$

$$H_x = \frac{H_x'}{\mu_e \sigma U_0 d H_0}, \qquad H_y = \frac{H_y'}{\mu_e \sigma U_0 d H_0}, \tag{14}$$

$$u_x = \frac{u_x'}{U_0}, \qquad u_y = \frac{u_y'}{U_0}, \tag{15}$$

$$h_x = \frac{h_x'}{\mu_e \sigma U_0 d H_0}, \qquad h_y = \frac{h_y'}{\mu_e \sigma U_0 d H_0}, \tag{16}$$

$$\eta = \frac{z}{d}, \qquad t = \frac{t'}{d^2/\upsilon}, \tag{17}$$

$$\omega = \frac{\omega'}{\upsilon/d^2} \tag{18}$$

Using the above, and since all the physical quantities are functions of z and t only, the Eqs. (1), (3) and (6) satisfies identically, and the Eqs. (2), (4), (5) and (7) after simplification reduce to the following in the dimensionless form.

For clear fluid region-I

$$\frac{\partial U_x}{\partial t} = \frac{\partial^2 U_x}{\partial \eta^2} + M^2 \cos\theta \frac{\partial H_x}{\partial \eta}, \tag{19}$$

$$\frac{\partial U_y}{\partial t} = \frac{\partial^2 U_y}{\partial \eta^2} + M^2 \cos\theta \frac{\partial H_y}{\partial \eta}, \tag{20}$$

$$\frac{\partial H_x}{\partial t} = \frac{1}{\mathrm{Pr}_m}\left[\frac{\partial^2 H_x}{\partial \eta^2} + m\cos\theta \frac{\partial^2 H_y}{\partial \eta^2} + \cos\theta \frac{\partial U_x}{\partial \eta}\right], \tag{21}$$

$$\frac{\partial H_y}{\partial t} = \frac{1}{\mathrm{Pr}_m}\left[\frac{\partial^2 H_y}{\partial \eta^2} - m\cos\theta \frac{\partial^2 H_x}{\partial \eta^2} + \cos\theta \frac{\partial U_y}{\partial \eta}\right], \tag{22}$$

For porous region-II

$$\frac{\partial u_x}{\partial t} = \phi \frac{\partial^2 u_x}{\partial \eta^2} + M^2 \cos\theta \frac{\partial h_x}{\partial \eta} - \frac{u_x}{k}, \tag{23}$$

$$\frac{\partial u_y}{\partial t} = \phi \frac{\partial^2 u_y}{\partial \eta^2} + M^2 \cos\theta \frac{\partial h_y}{\partial \eta} - \frac{u_y}{k}, \tag{24}$$

$$\frac{\partial h_x}{\partial t} = \frac{1}{\mathrm{Pr}_m}\left[\frac{\partial^2 h_x}{\partial \eta^2} + m\cos\theta \frac{\partial^2 h_y}{\partial \eta^2} + \cos\theta \frac{\partial u_x}{\partial \eta}\right], \tag{25}$$

$$\frac{\partial h_y}{\partial t} = \frac{1}{\mathrm{Pr}_m}\left[\frac{\partial^2 h_y}{\partial \eta^2} - m\cos\theta \frac{\partial^2 h_x}{\partial \eta^2} + \cos\theta \frac{\partial u_y}{\partial \eta}\right], \tag{26}$$

and the corresponding initial and boundary conditions become;

$$\text{For } t \le 0, \quad U_x = U_y = 0, \quad H_x = H_y = 0 \quad u_x = u_y = 0, \quad h_x = h_y = 0 \quad \text{for all } \eta \tag{27}$$

$$\text{For } t>0, \quad \text{at } \eta=0, \quad u_x=u_y=0, \quad h_x=h_y=0 \tag{28}$$

$$\text{at } \eta=a, \quad u_x=U_x, \quad \phi\frac{\partial u_x}{\partial \eta}=\frac{\partial U_x}{\partial \eta}, \quad u_y=U_y, \quad \phi\frac{\partial u_y}{\partial \eta}=\frac{\partial U_y}{\partial \eta} \tag{29}$$

$$h_x=H_x, \quad \frac{\partial h_x}{\partial \eta}=\frac{\partial H_x}{\partial \eta}, \quad h_y=H_y, \quad \frac{\partial h_y}{\partial \eta}=\frac{\partial H_y}{\partial \eta} \tag{30}$$

$$\text{at } \eta=1, \quad U_x=\cos\omega t, \quad U_y=0, \quad H_x=H_y=0 \tag{31}$$

where $a=a'/d$; $M=\mu_e H_0 d\sqrt{\sigma/\mu}$, the Hartmann number; $\mathrm{Pr}_m=\sigma\mu_e\upsilon$, the magnetic Prandtl number; $k=k_0/d^2$, the permeability parameter; and $\phi=\bar{\mu}/\mu$, the viscosity ratio parameter.

Method of solution

The following new variables are introduced.

$$F=U_x+iU_y, \tag{32}$$

$$H=H_x+iH_y, \tag{33}$$

$$\bar{F}=u_x+iu_y, \text{ and} \tag{34}$$

$$\bar{H}=h_x+ih_y. \tag{35}$$

Using above, the Eqs. (19) - (26) reduces to;

$$\frac{\partial F}{\partial t}=\frac{\partial^2 F}{\partial \eta^2}+M^2\cos\theta\frac{\partial H}{\partial \eta}, \tag{36}$$

$$\frac{\partial H}{\partial t}=\frac{1}{\mathrm{Pr}_m}\left[\left(1-im\cos\theta\right)\frac{\partial^2 H}{\partial \eta^2}+\cos\theta\frac{\partial F}{\partial \eta}\right], \tag{37}$$

$$\frac{\partial \bar{F}}{\partial t}=\phi\frac{\partial^2 \bar{F}}{\partial \eta^2}+M^2\cos\theta\frac{\partial \bar{H}}{\partial \eta}-\frac{\bar{F}}{k}, \tag{38}$$

$$\frac{\partial \bar{H}}{\partial t}=\frac{1}{\mathrm{Pr}_m}\left[\left(1-im\cos\theta\right)\frac{\partial^2 \bar{H}}{\partial \eta^2}+\cos\theta\frac{\partial \bar{F}}{\partial \eta}\right], \tag{39}$$

and the initial and boundary conditions (27) - (31) reduce to;

$$\text{For } t\le 0, \quad F=\bar{F}=0, \quad H=\bar{H}=0 \quad \text{for all } \eta \tag{40}$$

$$\text{For } t>0, \quad \text{at } \eta=0, \quad \bar{F}=\bar{H}=0 \tag{41}$$

$$\text{at } \eta=a, \quad \bar{F}=F, \quad \phi\frac{\partial \bar{F}}{\partial \eta}=\frac{\partial F}{\partial \eta} \tag{42}$$

$$\bar{H} = H, \quad \frac{\partial \bar{H}}{\partial \eta} = \frac{\partial H}{\partial \eta} \tag{43}$$

$$\text{at } \eta = 1, \quad F = \cos \omega t, \quad H = 0 . \tag{44}$$

Numerical solution

The Eqs. (36) - (39), subject to the initial and boundary conditions (40) - (44), are solved using the Crank-Nicolson implicit finite difference scheme, where the computational domain $(0 < t < \infty) \times (0 < \eta < 1)$ is divided into a mesh of straight lines, which are parallel to the t and η axes. On substitution of finite difference approximations to derivatives into Eqs. (36) - (39) and boundary conditions (40) - (44), the following set of algebraic equations are obtained.

$$F_{i,j} = \bar{F}_{i,j} = H_{i,j} = \bar{H}_{i,j} = 0, \qquad \text{for } j = 0, \quad i = 0,1,2,3,...n-1,n,n+1,...p \tag{45}$$

$$F_{0,j} = H_{0,j} = 0 \qquad \text{for } j = 1,2,3,..... \tag{46}$$

$$-\frac{\lambda\phi_1}{2} F_{i+1,j+1} + \left(\lambda\phi_1 + 1 + \frac{\Delta t}{2k}\right) F_{i,j+1} - \frac{\lambda\phi_1}{2} F_{i-1,j+1} - \frac{M^2 \cos\theta}{2} \lambda \Delta\eta \left(H_{i,j+1} - H_{i-1,j+1}\right)$$
$$= \frac{\lambda\phi_1}{2} F_{i+1,j} + \left(-\lambda\phi_1 + 1 - \frac{\Delta t}{2k}\right) F_{i,j} + \frac{\lambda\phi_1}{2} F_{i-1,j} + \frac{M^2 \cos\theta}{2} \lambda \Delta\eta \left(H_{i,j} - H_{i-1,j}\right)$$
$$\text{for } \; i = 1,2,...,(n-1), \;\; j = 0,1,2,3,..... \tag{47}$$

$$-\frac{\lambda}{2}\left(\frac{1 - im\cos\theta}{\mathrm{Pr}_m}\right) H_{i+1,j+1} + \left(\lambda\left(\frac{1 - im\cos\theta}{\mathrm{Pr}_m}\right) + 1\right) H_{i,j+1} - \frac{\lambda}{2}\left(\frac{1 - im\cos\theta}{\mathrm{Pr}_m}\right) H_{i-1,j+1}$$
$$- \frac{\cos\theta}{2\,\mathrm{Pr}_m} \lambda \Delta\eta \left(F_{i,j+1} - F_{i-1,j+1}\right) = \frac{\lambda}{2}\left(\frac{1 - im\cos\theta}{\mathrm{Pr}_m}\right) H_{i+1,j} + \left(-\lambda\left(\frac{1 - im\cos\theta}{\mathrm{Pr}_m}\right) + 1\right) H_{i,j}$$
$$+ \frac{\lambda}{2}\left(\frac{1 - im\cos\theta}{\mathrm{Pr}_m}\right) H_{i-1,j} + \frac{\cos\theta}{2\,\mathrm{Pr}_m} \lambda \Delta\eta \left(F_{i,j} - F_{i-1,j}\right)$$
$$\text{for } \; i = 1,2,...,(n-1), \;\; j = 0,1,2,3,..... \tag{48}$$

$$F_{n+1,j} - (\phi + 1) F_{n,j} + \phi F_{n-1,j} = 0 \qquad \text{for } j = 1,2,3,..... \tag{49}$$

$$H_{n+1,j} - 2H_{n,j} + H_{n-1,j} = 0 \qquad \text{for } j = 1,2,3,..... \tag{50}$$

$$-\frac{\lambda}{2} F_{i+1,j+1} + (\lambda + 1) F_{i,j+1} - \frac{\lambda}{2} F_{i-1,j+1} - \frac{M^2 \cos\theta}{2} \lambda \Delta\eta \left(H_{i,j+1} - H_{i-1,j+1}\right)$$
$$= \frac{\lambda}{2} F_{i+1,j} + (-\lambda + 1) F_{i,j} + \frac{\lambda}{2} F_{i-1,j} + \frac{M^2 \cos\theta}{2} \lambda \Delta\eta \left(H_{i,j} - H_{i-1,j}\right)$$
$$\text{for } \; i = n+1, n+2,...,(p-1), \;\; j = 0,1,2,3,..... \tag{51}$$

$$-\frac{\lambda}{2}\left(\frac{1-im\cos\theta}{\mathrm{Pr}_m}\right)H_{i+1,j+1}+\left(\lambda\left(\frac{1-im\cos\theta}{\mathrm{Pr}_m}\right)+1\right)H_{i,j+1}-\frac{\lambda}{2}\left(\frac{1-im\cos\theta}{\mathrm{Pr}_m}\right)H_{i-1,j+1}$$
$$-\frac{\cos\theta}{2\,\mathrm{Pr}_m}\lambda\Delta\eta\left(F_{i,j+1}-F_{i-1,j+1}\right)=\frac{\lambda}{2}\left(\frac{1-im\cos\theta}{\mathrm{Pr}_m}\right)H_{i+1,j}+\left(-\lambda\left(\frac{1-im\cos\theta}{\mathrm{Pr}_m}\right)+1\right)H_{i,j}$$
$$+\frac{\lambda}{2}\left(\frac{1-im\cos\theta}{\mathrm{Pr}_m}\right)H_{i-1,j}+\frac{\cos\theta}{2\,\mathrm{Pr}_m}\lambda\Delta\eta\left(F_{i,j}-F_{i-1,j}\right)$$
$$\text{for}\quad i=n+1,n+2,...,(p-1),\quad j=0,1,2,3,..... \tag{52}$$

$$F_{p,j}=\cos\left(\omega j\Delta t\right)\qquad \text{for } j=0,1,2,3,..... \tag{53}$$

$$H_{p,j}=0\qquad \text{for } j=0,1,2,3,..... \tag{54}$$

where, $n=a/\Delta\eta$; $p=1/\Delta\eta$; $\lambda=\Delta t/\Delta\eta^2$; $\Delta t,\Delta\eta$ are mesh sizes along time and space directions, respectively; and index *i* refers to space and *j* for time.

After some preliminary numerical experiments, the step sizes have been fixed, and the computational domain is divided into intervals with step sizes $\Delta t=0.0025$ and $\Delta\eta=0.01$ for time (t) and space η respectively. Computations are carried out by changing step sizes slightly (see **Table 1**), which do not show any significant change in the results for u_x and $(\tau_x)_{\eta=1}$ obtained by the numerical scheme. It is seen that the results for u_x and $(\tau_x)_{\eta=1}$ differ only in the sixth decimal place; thus, convergence of the scheme is assumed.

Table 1 (a) Values of u_x, (b) values of $(\tau_x)_{\eta=1}$, for $\phi = 1.25,\ k = 1,\ M = 5,\ \theta = \pi/3,\ \omega = \pi/2,\ m = 1,\ \mathrm{Pr}_m = 0.001$, t = 0.75, $\Delta\eta = 0.01$.

	ΔT			
η	0.0015	0.002	0.0025	0.003
0	0	0	0	0
0.1	0.057782	0.057782	0.057782	0.057782
0.2	0.107911	0.107911	0.107911	0.107911
0.3	0.162969	0.162969	0.162969	0.162969
0.4	0.210410	0.210410	0.210410	0.210410
0.5	0.251489	0.251489	0.251489	0.251489
0.6	0.287181	0.287181	0.287181	0.287181
0.7	0.318135	0.318135	0.318135	0.318135
0.8	0.344608	0.344608	0.344609	0.344609
0.9	0.366390	0.366390	0.366390	0.366390
1	0.382683	0.382683	0.382683	0.382683

(a)

ΔT	λ	$(\tau_x)_{\eta=1}$
0.001	10	0.134551
0.0015	15	0.134551
0.002	20	0.134551
0.0025	25	0.134556

(b)

Discussion

In this study, the numerical solution of the oscillatory hydromagnetic flow of a viscous electrically conducting fluid in a horizontal composite channel bounded above by an impermeable oscillating plate and below by a plate with porous layer perfectly attached to it is presented, in the presence of an oblique magnetic field. In this section, the effects of physical parameters on the flow fields of both regions are analyzed. Special attention is given to the effect of the permeability of the porous layer which is attached to the lower plate of the channel, the strength of the magnetic field, and the Hall current. A porous medium creates resistance to the viscous fluid flow, and thus affects the flow of the clear fluid region through the common boundary. The magnetic field suppresses the flow in the channel. In this study, the Hall effect is also taken into consideration, since it becomes important when the strength of the magnetic field is high or the collision frequency is low in an ionized gas. In such a case, the electromagnetic force causes an isotropic electrical conductivity in the plasma, which produces a current (Hall current) in the flow, normal to both magnetic and electric fields. It causes a secondary flow by interacting with the applied magnetic field in the channel.

The velocity profiles in the primary and secondary directions are shown in **Figures 2 - 12**. Numerical evaluations for the primary velocity component are shown in **Figure 2**. It clearly exhibits oscillatory flow distribution for various values of ωt. **Figure 3** presents profiles of the velocity component in the primary direction (u_x) for various values of time *t*, keeping all other data fixed

as $\phi = 1.25,\ k = 1,\ M = 5,\ \theta = \pi/3,\ \omega = \pi/2,\ m = 1,\ \mathrm{Pr}_m = 0.001$. It is seen that, with increasing t values, the flow is accelerated across the channel. Due to the oscillating plate there is a non-zero primary velocity at the upper wall $(\eta = 1)$, while the velocity vanishes at the lower stationary wall. Profiles of velocity component u_x are plotted in **Figures 4 - 8** at a fixed time in the flow. These figures show the effects of the physical parameters, permeability (k), viscosity ratio (ϕ), magnetic field (M), orientation of the applied magnetic field (θ) and Hall current parameter (m) respectively on the primary flow distribution in the channel. It is noticed in **Figure 4** that the effect of the permeability (k) of the porous layer is to enhance the primary velocity (u_x) across the channel. With an increase in *k* the Darcian resistance term, $-\frac{1}{k}u_x$, is reduced in the primary flow momentum equation, causing flow acceleration. In fact, with increasing *k* values, the flow regime will become increasingly permeable and less resistance will be offered to the primary flow. However, **Figure 5** shows that viscosity ratio (ϕ) reduces it. Thus the presence of a porous layer exerts a regulatory effect on the primary flow and therefore can be exploited as a useful control mechanism in the channel. With increasing *M* values, **Figure 6** shows that the primary flow is decelerated in the upper half-space of the channel, because Lorentz force due to magnetic field produces resistance to the flow. However, it is accelerated in the porous layer and its nearby region. For a constant *M* value, the magnetohydrodynamic drag will be minimum when $\theta = \pi/2$ and maximum when $\theta = 0$, hence in **Figure 7** it is seen that as θ increases from the value 0 through $\pi/6$, $\pi/4$, $\pi/3$, and to $\pi/2$, the hydromagnetic drag force continuously reduces, and hence primary flow accelerates in the upper half-space. Primary flow also enhances near the upper plate with the increase in the Hall current parameter (m), but its effect is insignificant in the lower part of the channel.

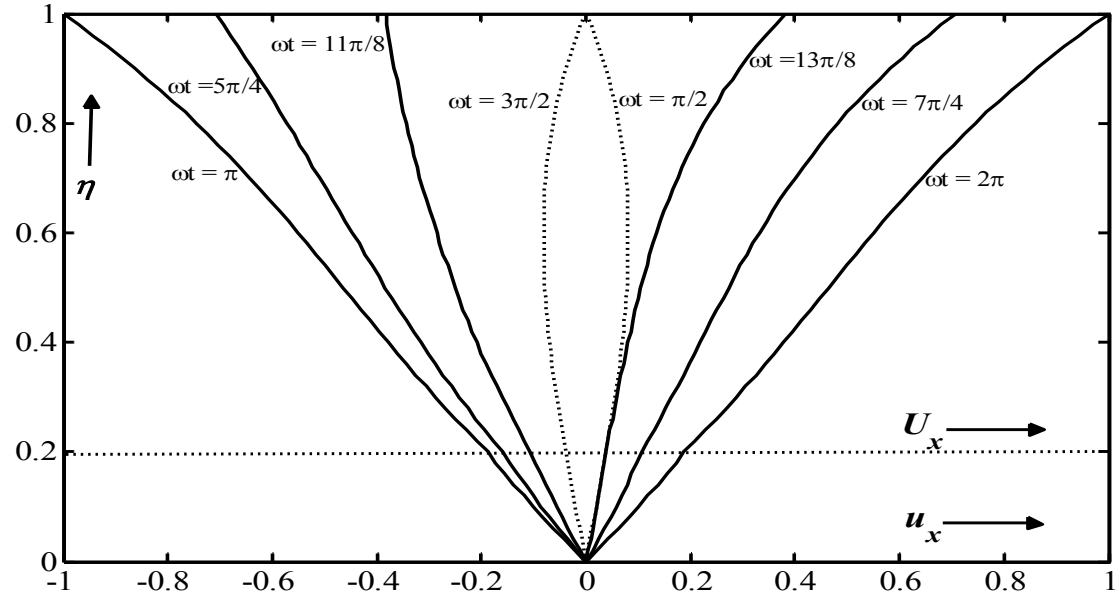

Figure 2 Velocity profiles in primary direction (u_x) for $\phi = 1.25,\ k = 1,\ M = 5,\ \theta = \pi/3,\ \omega = \pi/2,\ m = 1,\ \mathrm{Pr}_m = 0.001$.

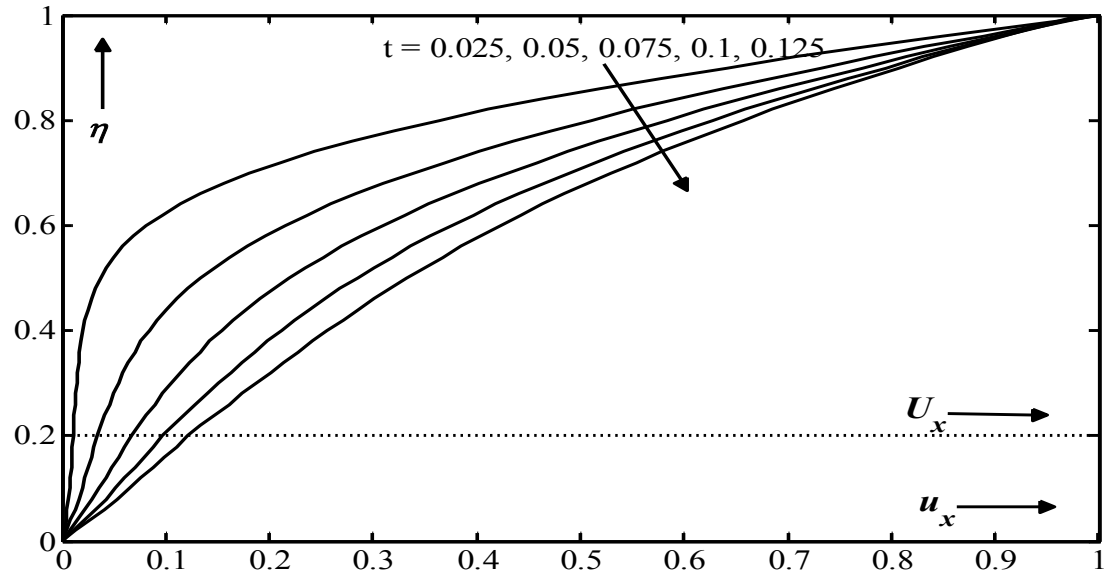

Figure 3 Velocity profiles in primary direction (u_x) for $\phi = 1.25,\ M = 5,$ k =1, $\theta = \pi/3,\ \omega = \pi/2,$ $m = 1,\ \mathrm{Pr}_m = 0.001$.

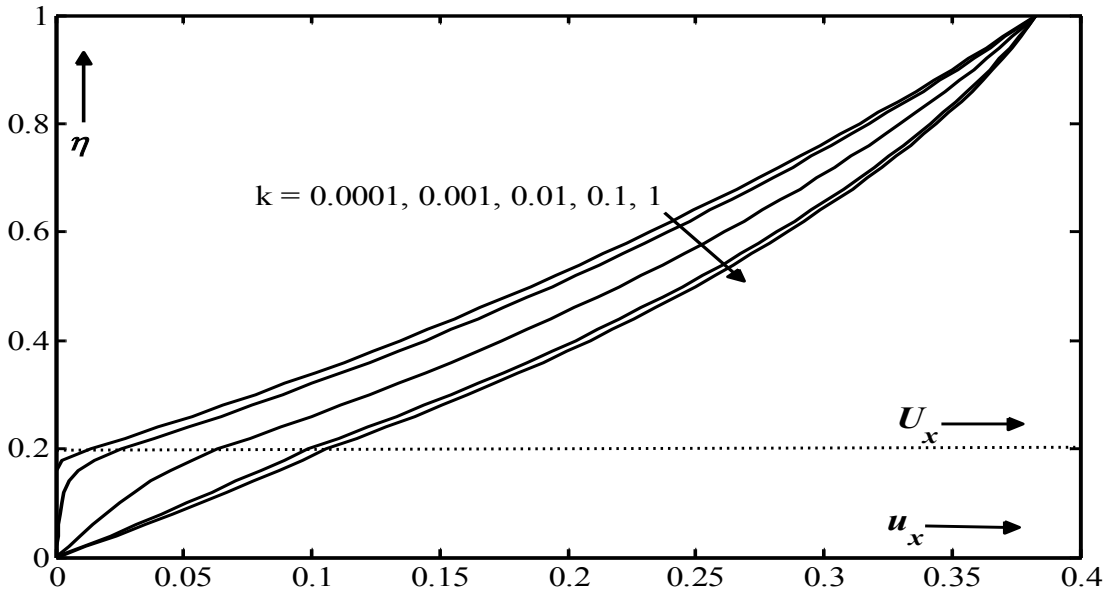

Figure 4 Velocity profiles in primary direction (u_x) for $\phi = 1.25,\ M = 5,\ \theta = \pi/3,$ $\omega = \pi/2,\ m = 1,\ \mathrm{Pr}_m = 0.001,\ t = 0.75$.

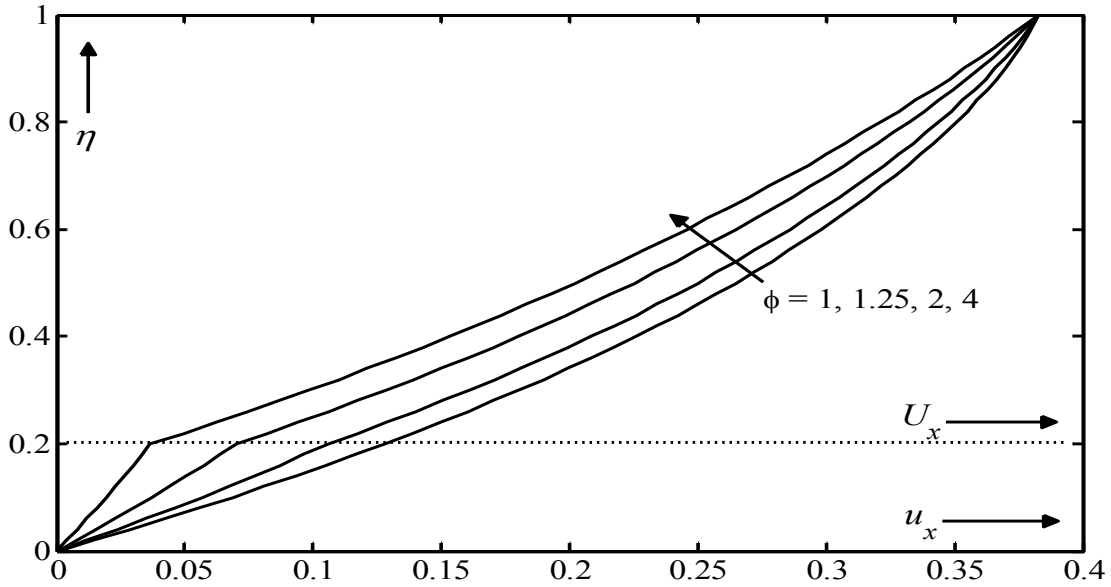

Figure 5 Velocity profiles in primary direction (u_x) for k =1, $M = 5$, $\theta = \pi/3$, $\omega = \pi/2$, $m = 1$, $\mathrm{Pr}_m = 0.001$, $t = 0.75$.

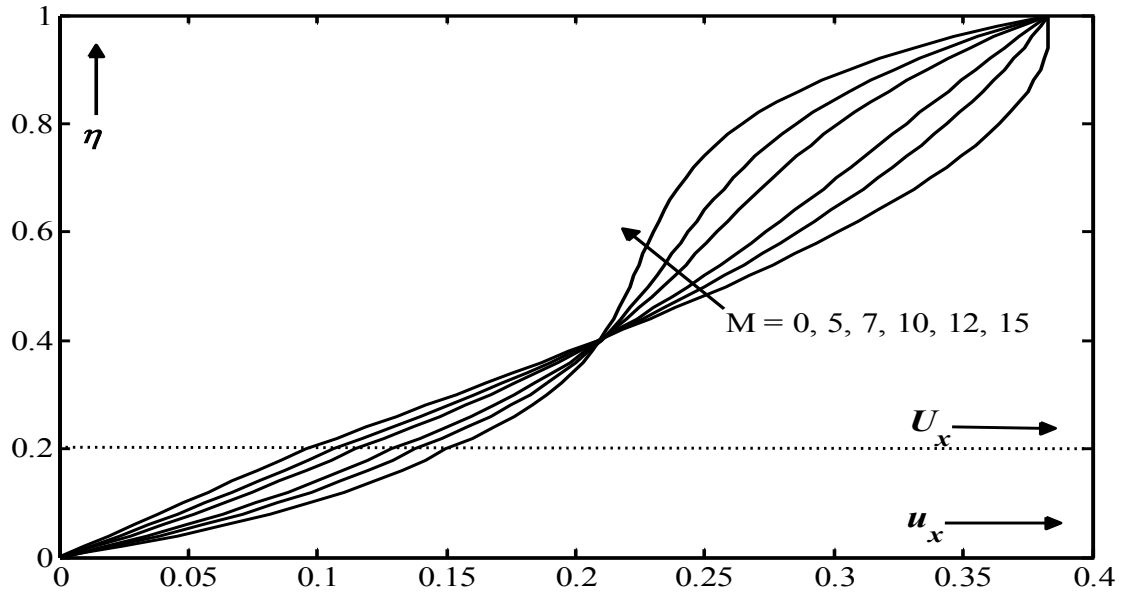

Figure 6 Velocity profiles in primary direction (u_x) for $\phi = 1.25$, $\theta = \pi/3$, $\omega = \pi/2$, $k = 1$, $m = 1$, $\mathrm{Pr}_m = 0.001$, $t = 0.75$.

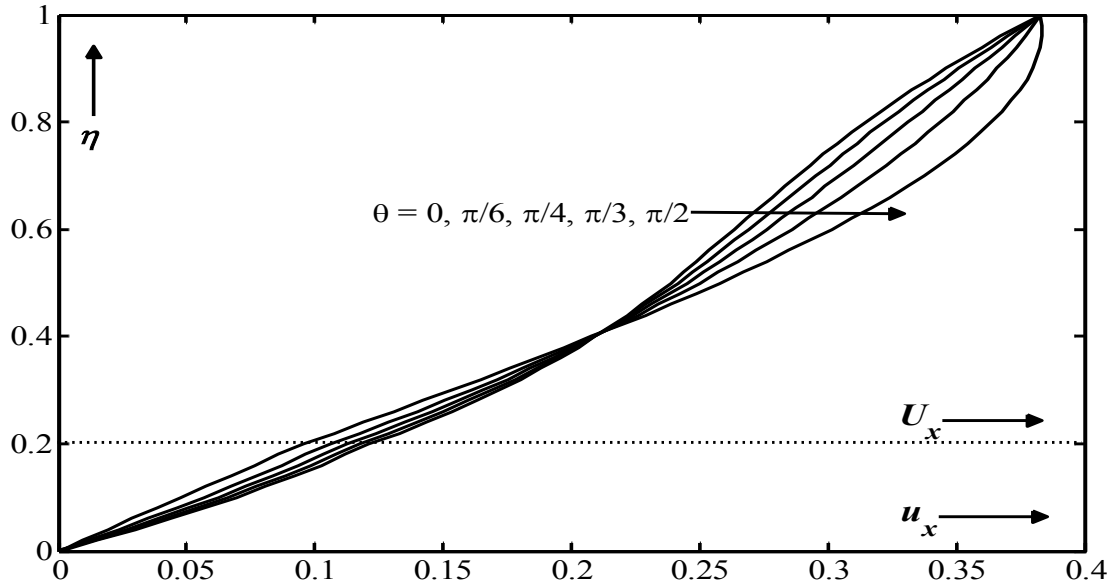

Figure 7 Velocity profiles in primary direction (u_x) for $\phi = 1.25,\ M = 5,\ \omega = \pi/2,\ k = 1,\ m = 1,$ $\mathrm{Pr}_m = 0.001,\ t = 0.75$.

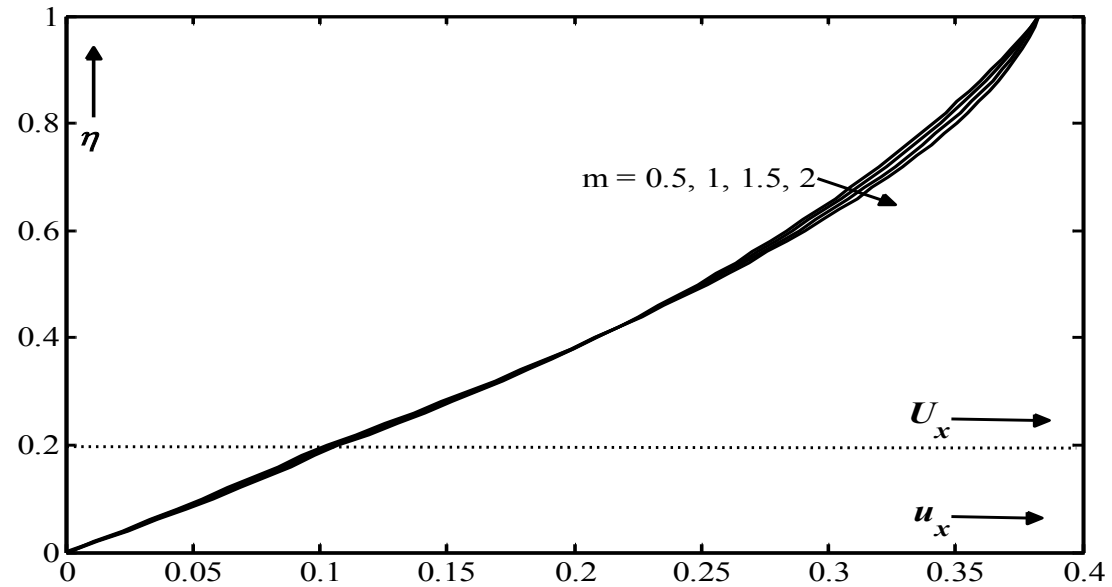

Figure 8 Velocity profiles in primary direction (u_x) for $\phi = 1.25,\ M = 5,\ \theta = \pi/3,\ ,\ \omega = \pi/2,\ k = 1,$ $\mathrm{Pr}_m = 0.001$, $t = 0.75$

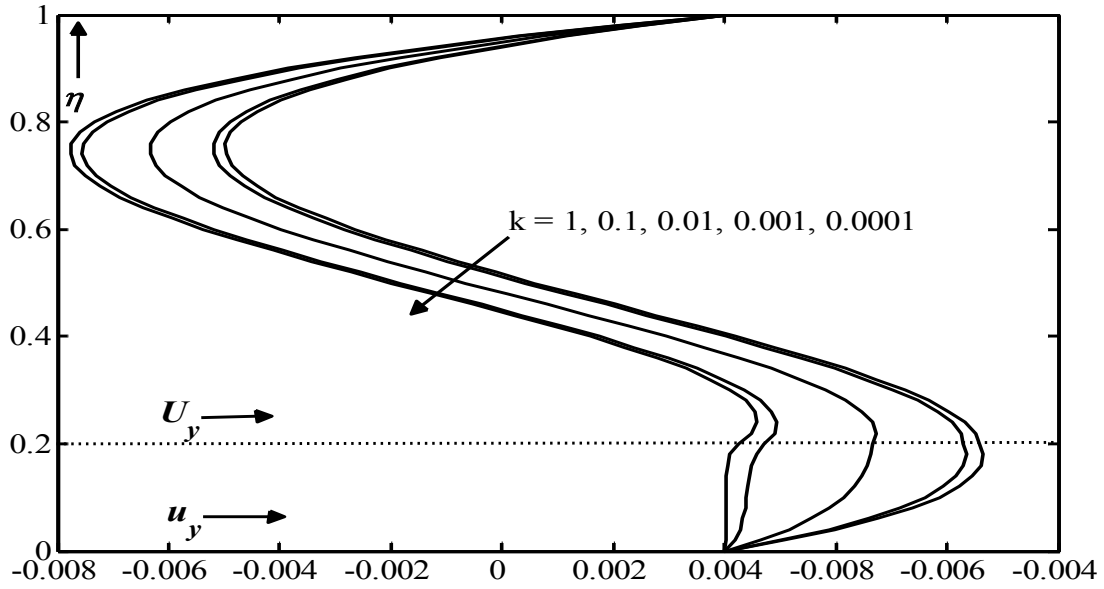

Figure 9 velocity profiles in secondary direction $\left(u_y\right)$ for $\phi = 1.25,\ M = 5,\ \theta = \pi/3,\ \ \omega = \pi/2,\ m = 1,$ $\mathrm{Pr}_m = 0.001,\ t = 0.75$.

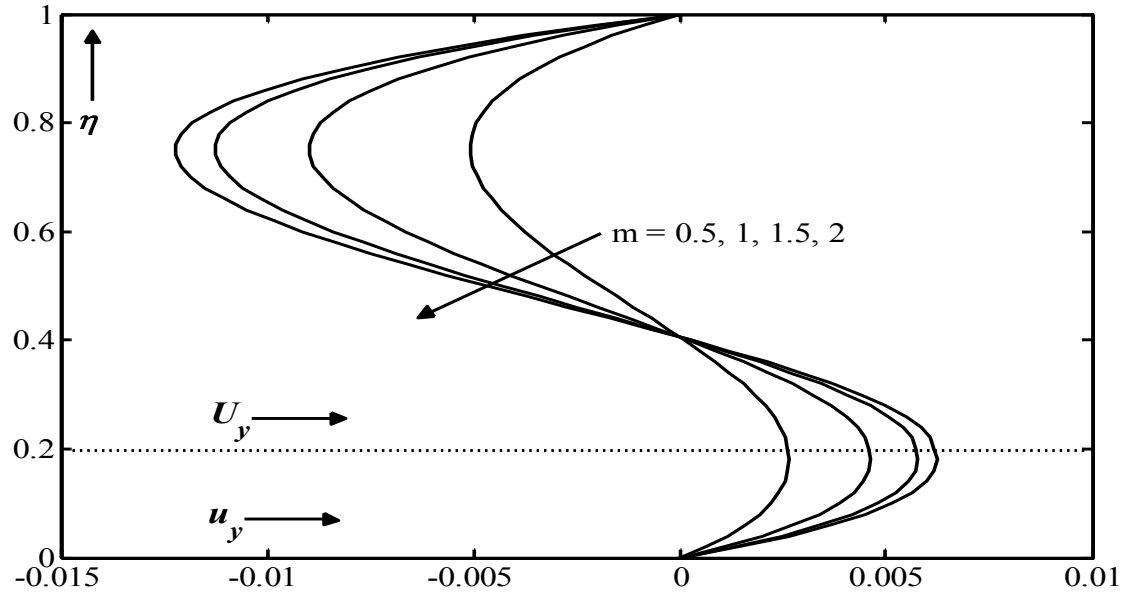

Figure 10 velocity profiles in secondary direction $\left(u_y\right)$ for $\phi = 1.25,\ M = 5,\ \theta = \pi/3,\ \omega = \pi/2,\ k = 1,$ $\mathrm{Pr}_m = 0.001,\ t = 0.75$.

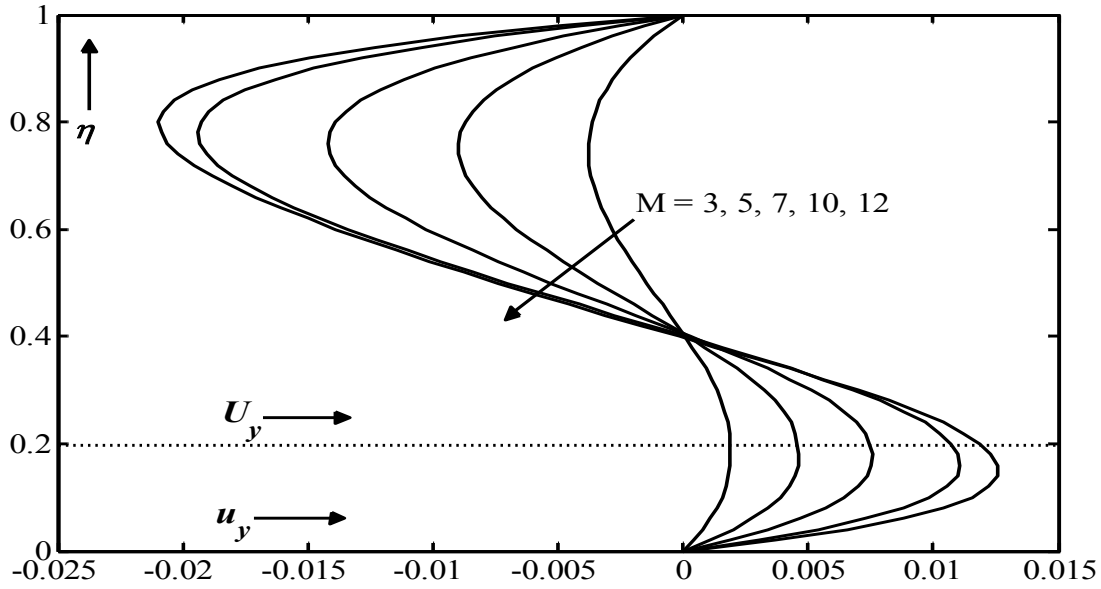

Figure 11 velocity profiles in secondary direction $\left(u_y\right)$ for $\phi = 1.25,\ \theta = \pi/3,\ \omega = \pi/2,\ k = 1,\ m = 1,\ \mathrm{Pr}_m = 0.001,\ t = 0.75$.

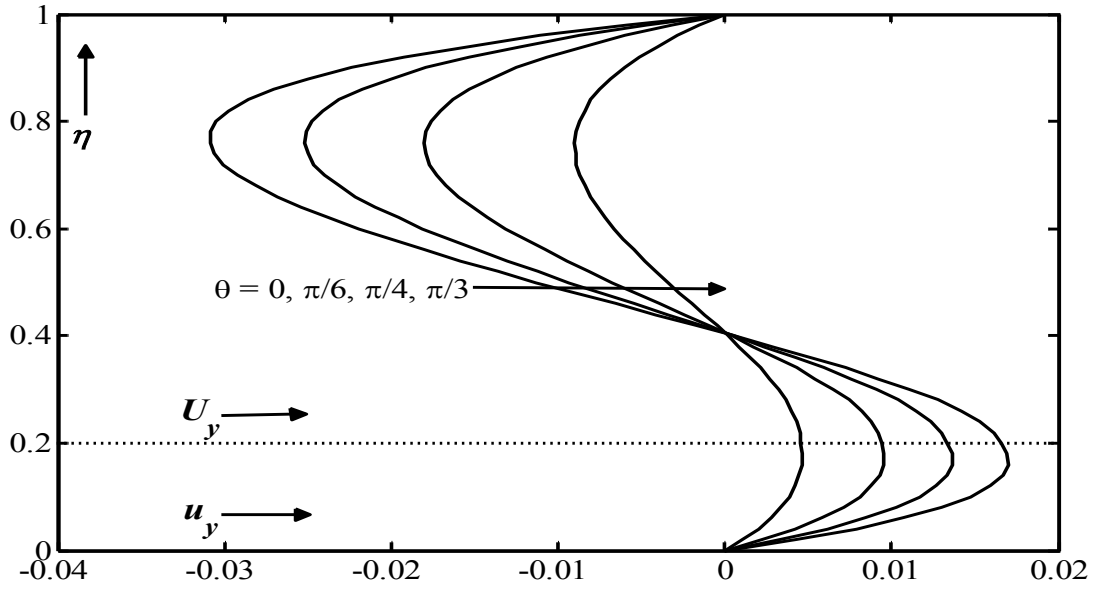

Figure 12 velocity profiles in secondary direction $\left(u_y\right)$ for $\phi = 1.25,\ M = 5,\ \omega = \pi/2,\ k = 1,\ m = 1,\ \mathrm{Pr}_m = 0.001,\ t = 0.75$.

Figures 9 - 12 show profiles of the velocity component u_y in the secondary direction for various values of the physical parameters. It is noticed in these figures that the velocity profiles are negative in the upper part of the channel and positive in the lower part. The permeability parameter (k) accelerates u_y in the lower part of the channel, since the resistance of the porous medium particles to the secondary flow will be lowered as *k* increases; however, it decelerates in the upper part. The secondary velocity is caused by the Hall current effect; therefore, as the parameter *m* increases, u_y also increases. The magnetic field parameter (M) also increases the secondary velocity in the channel. Because secondary flow is due to the Hall effect, which is caused by the strong magnetic field, it is seen that as θ increases, the hydromagnetic force decreases, which serves to decelerate the secondary velocity.

Figures 13 and **14** show variations of the induced magnetic fields H_x and H_y in the primary and secondary flow directions respectively, for various values of the physical parameters *k*, ϕ, *M* and *m*. It is found in **Figure 13** that the effect of the permeability parameter (k) is to reduce H_x in the clear fluid region, while the effect of this parameter is insignificant in the porous region. However, the effect of the Hall current (m) or the magnetic field (M) is to reduce H_x throughout the channel. The viscosity ratio parameter (ϕ) increases H_x in the clear fluid region. **Figure 14** shows that with the increase in permeability parameter (k), H_y decreases in the clear fluid region, while in the porous region it increases slightly. However, the reverse effect is observed with the increase in viscosity ratio parameter (ϕ). The magnetic field (M) reduces H_y throughout the channel and the reverse effect is observed with the increase in the Hall current parameter (m).

The graphs of the shear stresses $(\tau_x)_{\eta=1}$ and $(\tau_y)_{\eta=1}$ at the upper oscillating plate of the channel in the primary and secondary flow directions have been plotted in **Figures 15** and **16** respectively to see the effects of the applied magnetic field, and the permeability of the porous medium layer attached to the lower stationary plate. It is seen that the effect of the permeability (k) is to decrease the magnitude of both τ_x and τ_y, while both these shear stresses increase with the increase of magnetic field *M*. However, the effect of the Hall current parameter (m) is to decrease τ_x, while it increases τ_y.

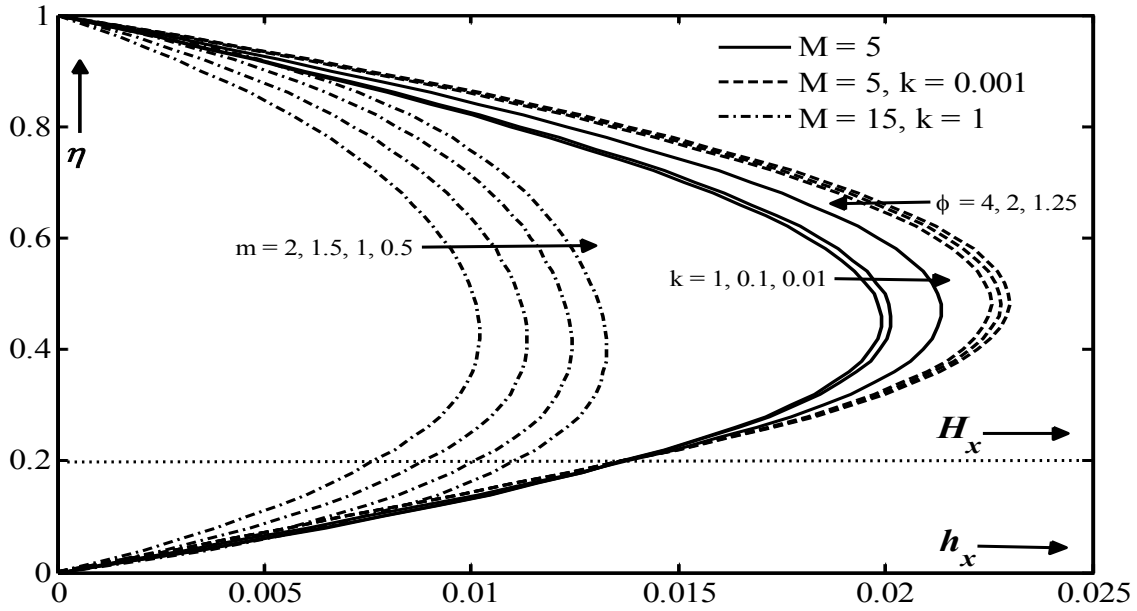

Figure 13 H_x for $\phi = 1.25,\ \theta = \pi/3,\ \ \omega = \pi/2,\ m = 1,\ \mathrm{Pr}_m = 0.001\ t = 0.75$.

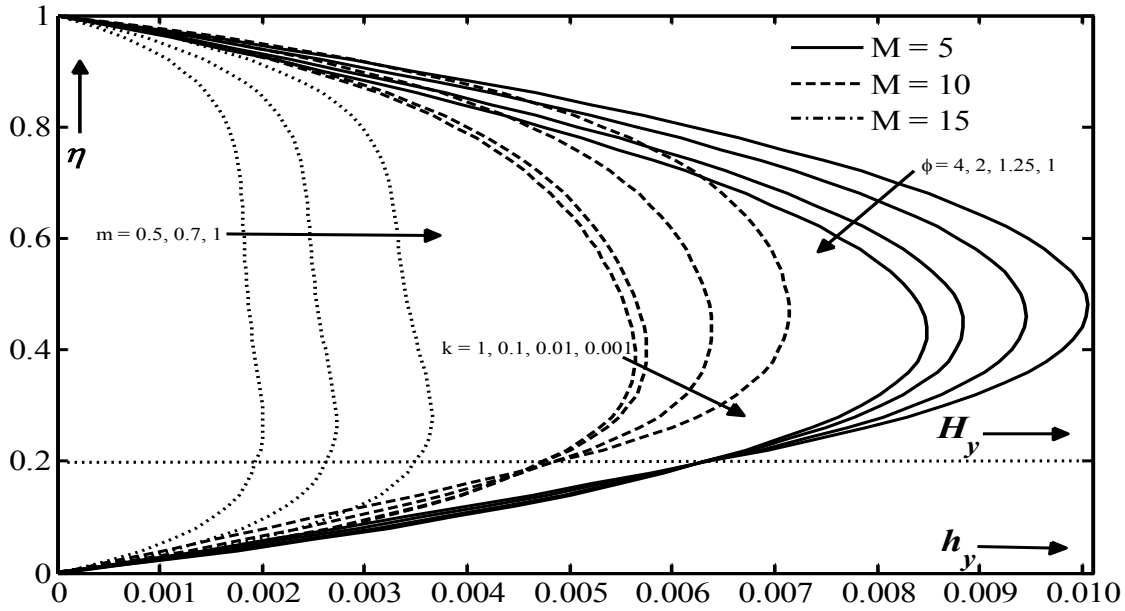

Figure 14 H_y for $\phi = 1.25,\ \theta = \pi/3,\ \ \omega = \pi/2,\ m = 1,\ \mathrm{Pr}_m = 0.001,\ t = 0.75$.

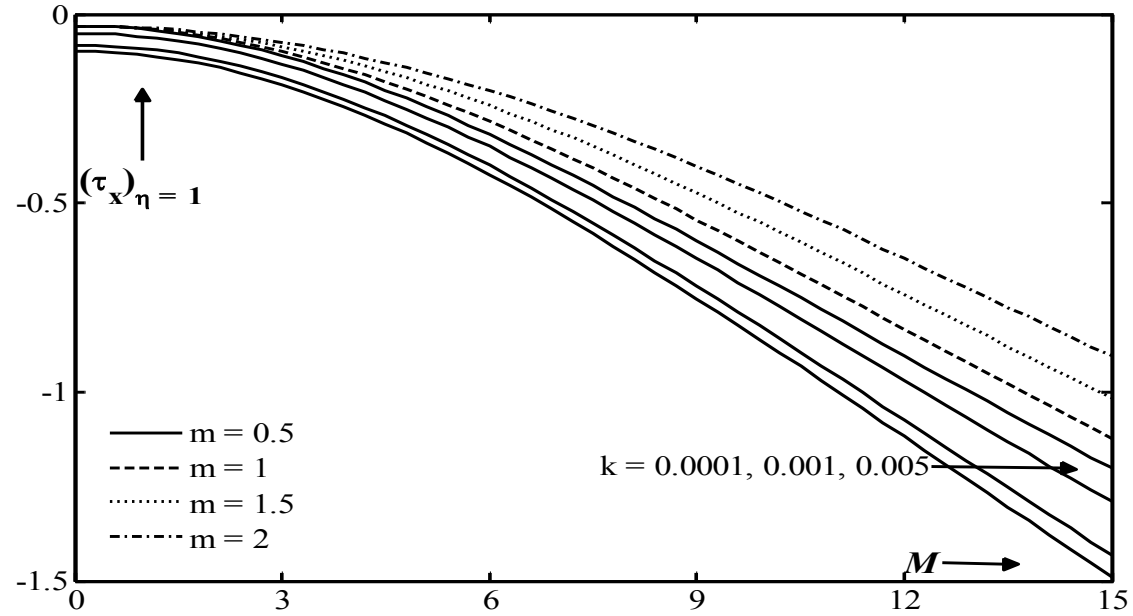

Figure 15 Shear stress at the oscillating wall $(\tau_x)_{\eta=1}$ vs M for $\phi = 1.25,\ \theta = \pi/3,\ \ \omega = \pi/2,\ k = 0.01,$ $\mathrm{Pr}_m = 0.001,\ t = 0.75$.

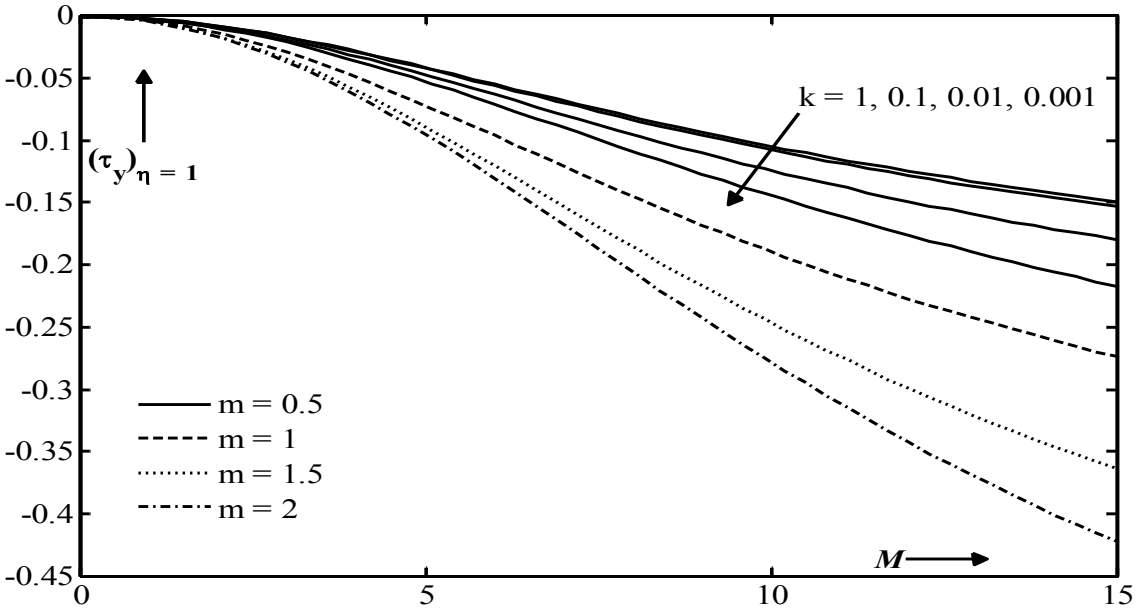

Figure 16 Shear stress at the oscillating wall $(\tau_y)_{\eta=1}$ vs M for $\phi = 1.25,\ \theta = \pi/3,\ \ \omega = \pi/2,\ k = 1,$ $\mathrm{Pr}_m = 0.001,\ t = 0.75$.

Conclusions

This type of viscous fluid flow occurs in fluid machinery involving moving parts, and this study is especially important for predicting the MHD flow in such settings, where the regime may be a composite channel with an oblique magnetic field. Oscillatory hydromagnetic flows in such channels have applications in material processing, biomechanics, vibrating media, MHD energy generator systems and astrophysical flows. The present study thus finds possible applications in, for example, fluid engineering exploiting porous materials, and in hybrid designs for chemical engineering processes.

Acknowledgement

The authors wish to express their thanks to the reviewers for their helpful comments and suggestions to improve the quality and presentation of this paper. The support provided by the Council of Scientific and Industrial Research through Senior Research Fellowship to Rashmi Agrawal, one of the authors, is gratefully acknowledged.

References

[1] C Beckermann, S Ramadhyani and R Viskanta. Natural convection flow and heat transfer between a fluid layer and a porous layer inside a rectangular enclosure. *J. Heat Tran.* 1987; **109**, 363-70.
[2] WJ Chang and WL Chang. Mixed convection in a vertical parallel-plate channel partially filled with porous media of high permeability. *Int. J. Heat Mass Tran.* 1996; **39**, 1331-42.
[3] OM Haddad. Fully developed free convection in open-ended vertical channels partially filled with porous material. *J. Porous Media* 1999; **2**, 179-89.
[4] MK Alkam, MA Al-Nimr and MO Hamdan. On forced convection in channels partially filled with porous substrates. *Heat Mass Tran.* 2002; **38**, 337-42.
[5] MA Al-Nimr and AF Khadrawi. Transient free convection fluid flow in domains partially filled with porous media. *Tran. Porous Media* 2003; **51**, 157-72.
[6] A Nakayama. Non-Darcy Couette flow in a porous medium filled with an inelastic non-Newtonian fluid. *ASME J. Fluid Eng.* 1992; **114**, 642-7.
[7] DS Chauhan and KS Shekhawat. Heat transfer in Couette flow of a compressible Newtonian fluid in the presence of a naturally permeable boundary. *J. Phys. D: Appl. Phys*. 1993; **26**, 933-6.
[8] DS Chauhan and P Vyas. Heat transfer in hydromagnetic Couette flow of compressible Newtonian fluid. *ASCE J. Eng. Mech*. 1995; **121**, 57-61.
[9] AV Kuznetsov. Analytical investigation of Couette flow in a composite channel partially filled with a porous medium and partially with a clear fluid. *Int. J. Heat Mass Tran.* 1998; **41**, 2556-60.
[10] JA Ochoa-Tapia and S Whitaker. Momentum transfer at the boundary between a porous medium and a homogeneous fluid-I. Theoretical development. *Int. J. Heat Mass Tran.* 1995; **38**, 2635-46.
[11] JA Ochoa-Tapia and S Whitaker. Momentum transfer at the boundary between a porous medium and a homogeneous fluid-II. Comparison with experiment. *Int. J. Heat Mass Tran.* 1995; **38**, 2647-55.
[12] W Marques Jr., GM Kremer and FM Sharipov. Couette flow with slip and jump boundary conditions. *Continuum Mech. Thermodynam*. 2000; **12**, 379-86.
[13] ARA Khaled and K Vafai. The effect of the slip condition on Stokes and Couette flows due to an oscillating wall: exact solutions. *Int. J. Nonlinear Mech*. 2004; **39**, 795-809.
[14] OA Bég, HS Takhar, J Zueco, A Sajid and R Bhargava. Transient Couette flow in a rotating non-Darcian porous medium parallel plate configuration: network simulation method solutions. *Acta Mech*. 2008; **200**, 129-44.
[15] M Guria, S Das, RN Jana and SK Ghosh. Oscillatory Couette flow in the presence of an inclined magnetic field. *Meccanica* 2009; **44**, 555-64.
[16] DS Chauhan and V Kumar. Heat transfer effects in a Couette flow through a composite channel partly filled by a porous medium with a transverse sinusoidal injection velocity and heat source. *Therm. Sci.* 2011; **15**, S175-S186.

[17] DS Chauhan and V Kumar. Radiation effects on unsteady flow through a channel filled by a porous medium with velocity and temperature slip boundary conditions. *Appl. Math. Sci.* 2012; **6**, 1759-69.
[18] JD McWhirter, ME Crawford, DE Klein and TL Sanders. Model for inertialess magnetohydrodynamic flow in packed beds. *Fusion Sci. Tech.* 1998; **33**, 22-30.
[19] JD McWhirter, ME Crawford and DE Klein. Magnetohydrodynamic flows in porous media II: Experimental results. *Fusion Sci. Tech.* 1998; **34**, 187-97.
[20] DA Nield. Modeling the effects of a magnetic field or rotation on flow in a porous medium: momentum equation and anisotropic permeability analogy. *Int. J. Heat Mass Tran.* 1999; **42**, 3715-8.
[21] C Geindreau and JL Auriault. Magnetohydrodynamic flows in porous media. *J. Fluid Mech*. 2002; **466**, 343-63.
[22] DV Krishna, DRVP Rao and ASR Murthy. Hydromagnetic convection flow through a porous medium in a rotating channel. *J. Eng. Phys. Thermophys*. 2002; **75**, 281-91.
[23] T Hayat, SB Khan and M Khan. The influence of Hall current on the rotating oscillating flows of an Oldroyd-B fluid in a porous medium. *Nonlinear Dynamics* 2007; **47**, 353-62.
[24] T Hayat, SB Khan, M Sajid and S Asghar. Rotating flow of a third grade fluid in a porous space with Hall current. *Nonlinear Dynamics* 2007; **49**, 83-91.
[25] T Hayat, M Husain and M Khan. Effects of Hall current on flows of a Burger's fluid through a porous medium. *Tran. Porous Med*. 2007; **68**, 249-63.
[26] T Hayat, M Javed and N Ali. MHD peristaltic transport of a Jeffery fluid in a channel with compliant walls and porous space. *Tran. Porous Media* 2008; **74**, 259-74.
[27] OA Bég, L Sim, J Zueco and R Bhargava. Numerical study of magnetohydrodynamic viscous plasma flow in rotating porous media with Hall currents and inclined magnetic field influence. *Commun. Nonlinear Sci. Numer. Simulat.* 2010; **15,** 345-59.
[28] DS Chauhan and P Rastogi. Hall current and heat transfer effects on MHD flow in a channel partially filled with a porous medium in a rotating system. *Turk. J. Eng. Environ. Sci.* 2009; **33**, 167-84.
[29] DS Chauhan and R Agrawal. Effects of Hall current on MHD flow in a rotating channel partially filled with a porous medium. *Chem. Eng. Commun.* 2010; **197**, 830-45.
[30] DS Chauhan and R Agrawal. Effects of Hall current on MHD Couette flow channel partially filled with a porous medium in a rotating system. *Meccanica* 2012; **47**, 405-21.
[31] TG Cowling. *Magnetohydrodynamics*. Inter Science, New York, 1957.